Low nitrous oxide production through nitrifier-denitrification in intermittent-feed high-rate nitritation reactors

Su, Qingxian; Ma, Chun; Domingo-Felez, Carlos; Kiil, Anne Sofie; Thamdrup, Bo; Jensen, Marlene Mark; Smets, Barth F.

Published in:
Water Research

Link to article, DOI:
10.1016/j.watres.2017.06.067

Publication date:
2017

Document Version
Peer reviewed version

Accepted Manuscript

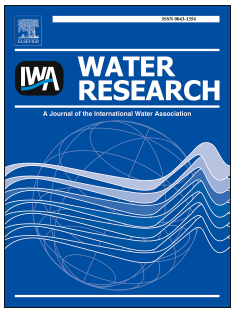

Low nitrous oxide production through nitrifier-denitrification in intermittent-feed high-rate nitritation reactors

Qingxian Su, Chun Ma, Carlos Domingo-Félez, Anne Sofie Kiil, Bo Thamdrup, Marlene Mark Jensen, Barth F. Smets

PII: S0043-1354(17)30528-6

DOI: 10.1016/j.watres.2017.06.067

Reference: WR 13022

To appear in: *Water Research*

Received Date: 7 February 2017

Revised Date: 24 May 2017

Accepted Date: 19 June 2017

Please cite this article as: Su, Q., Ma, C., Domingo-Félez, C., Kiil, A.S., Thamdrup, B., Jensen, M.M., Smets, B.F., Low nitrous oxide production through nitrifier-denitrification in intermittent-feed high-rate nitritation reactors, *Water Research* (2017), doi: 10.1016/j.watres.2017.06.067.

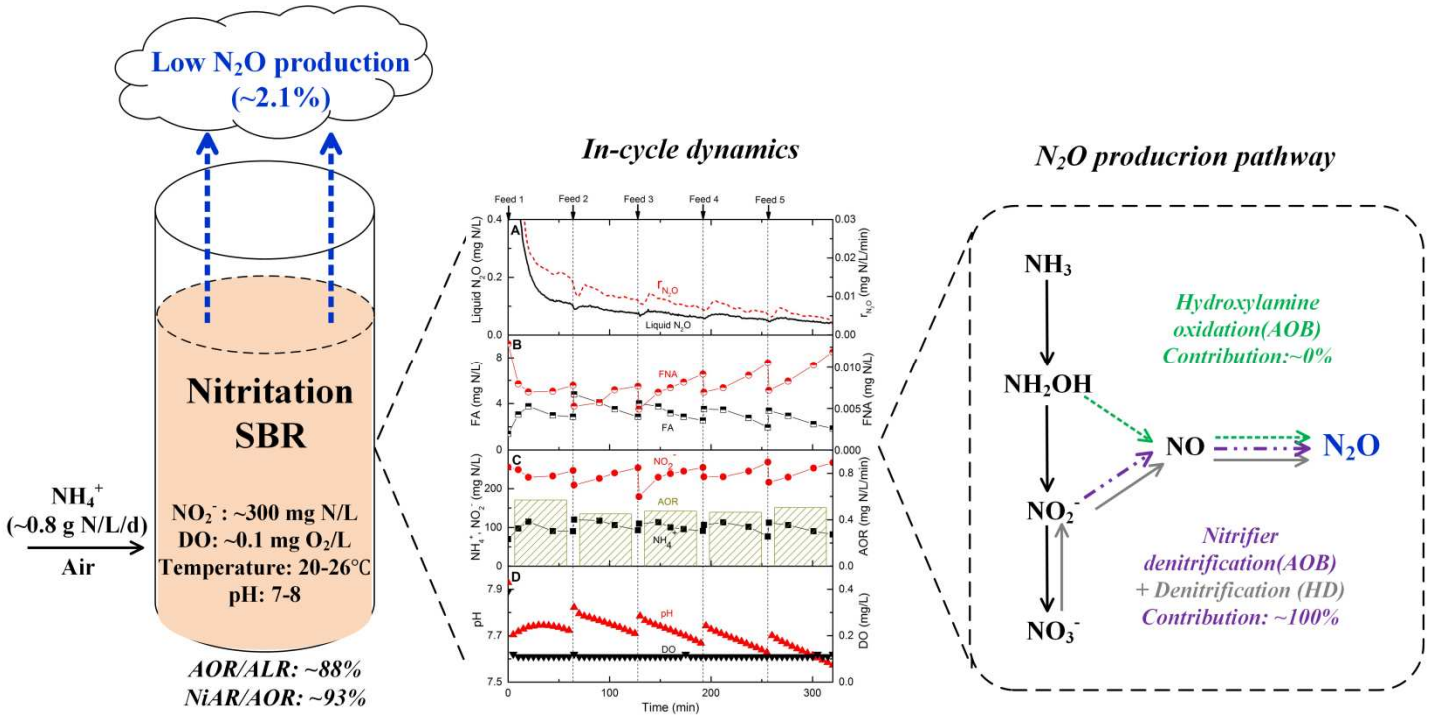

Low nitrous oxide production through nitrifier-denitrification in intermittent-feed high-rate nitritation reactors

Qingxian Su [a], Chun Ma [b], Carlos Domingo-Félez [a], Anne Sofie Kiil [a], Bo Thamdrup [b], Marlene Mark Jensen [a *], Barth F. Smets [a]

[a] *Department of Environmental Engineering, Technical University of Denmark, 2800 Lyngby, Denmark*

[b] *Nordic Center for Earth Evolution and Institute of Biology, University of Southern Denmark, 5230 Odense M, Denmark*

** Corresponding author.*

E-mail address: mmaj@env.dtu.dk

Abstract

Nitrous oxide (N_2O) production from autotrophic nitrogen conversion processes, especially nitritation systems, can be significant, requires understanding and calls for mitigation. In this study, the rates and pathways of N_2O production were quantified in two lab-scale sequencing batch reactors operated with intermittent feeding and demonstrating long-term and high-rate nitritation. The resulting reactor biomass was highly enriched in ammonia-oxidizing bacteria, and converted ~93 ± 14% of the oxidized ammonium to nitrite. The low DO set-point combined with intermittent feeding was sufficient to maintain high nitritation efficiency and high nitritation rates at 20-26 °C over a period of ~300 days. Even at the high nitritation efficiencies, net N_2O production was low (~2% of the oxidized ammonium). Net N_2O production rates transiently increased with a rise in pH after each feeding, suggesting a potential effect of pH on N_2O production. In situ application of ^{15}N labeled substrates revealed nitrifier denitrification as the dominant pathway of N_2O production. Our study highlights operational conditions that minimize N_2O emission from two-stage autotrophic nitrogen removal systems.

Keywords: Nitrous oxide; Nitritation; Ammonia-oxidizing bacteria; Intermittent feeding; pH; Nitrifier denitrification

1. Introduction

Autotrophic nitrogen removal by combined partial nitritation (PN, aerobic ammonium (NH_4^+) oxidation to nitrite (NO_2^-)) and anammox (anaerobic NH_4^+ oxidation with NO_2^- to dinitrogen gas (N_2)) is being implemented as an energy and resource-efficient process compared to traditional nitrification and heterotrophic denitrification process (Siegrist et al., 2008; Wett et al., 2013). Autotrophic nitrogen removal can be achieved either in one- or two-stage systems. Although the two-stage process requires higher investment costs related to the construction, this configuration allows for coordination and optimization of the individual conversion stages (Desloover et al., 2011). The PN-anammox process offers a promising alternative for nitrogen removal that meets both lower energy consumption, mainly due to lower aeration need, and lower carbon footprint emission without requirement for external carbon addition (Kartal et al., 2010). Nitritation can be achieved by manipulating operation parameters, such as low dissolved oxygen (DO) and high NH_4^+ loadings, that are favorable for ammonia-oxidizing bacteria (AOB) over nitrite-oxidizing bacteria (NOB) (Blackburne et al., 2008; Vadivelu et al., 2007). However, low DO and high NH_4^+ as well as high accumulation of NO_2^- produced by AOB in two-stage systems may promote accumulation and emission of nitrous oxide (N_2O) (Kampschreur et al., 2008; Kim et al., 2010; Mampaey et al., 2016; Peng et al., 2015, 2014; Tallec et al., 2006).

The ongoing accumulation of N_2O in the atmosphere (~0.3% per year) is of great concern because it contributes to global warming (N_2O has a ca. 300 times higher global warming potential than CO_2) and the destruction of stratospheric ozone (IPCC, 2013; Strokal and Kroeze, 2014). Indeed, documented N_2O emissions of up to 17% of the NH_4^+ oxidized from both lab-scale and full-scale PN reactors have been higher compared to measurements from conventional nitrification-denitrification processes (Desloover et al., 2011; Gao et al., 2016; Kong et al., 2013; Lv et al., 2016; Mampaey et al., 2016). The variation in N_2O emissions might be explained by the different

responses of N_2O production and consumption pathways to different operation strategies (e.g. feeding and aeration pattern) and parameters (e.g. NH_4^+, NO_2^-, DO and pH) (Burgess et al., 2002; Domingo-Félez et al., 2014; Law et al., 2011; Rathnayake et al., 2015; Schneider et al., 2014). There are two main pathways involved in N_2O produced by AOB: (a) the reduction of NO_2^- to N_2O via nitric oxide (NO), known as nitrifier denitrification (ND) (Ishii et al., 2014; Kim et al., 2010; Wrage et al., 2001) and (b) N_2O as a side product during incomplete oxidation of hydroxylamine (NH_2OH) to NO_2^- (Law et al., 2012; Poughon et al., 2001; Tallec et al., 2006), known as hydroxylamine oxidation. Furthermore, denitrifying bacteria can be as important as AOB in the production of N_2O under very low C/N conditions (Domingo-Félez et al., 2017). During heterotrophic denitrification (HD), N_2O is an obligate intermediate and is produced during incomplete denitrification. The exact biological pathways and environmental controls of N_2O production in two-staged autotrophic nitrogen removal systems still remains to be quantified (Ishii et al., 2014; Law et al., 2012; Terada et al., 2017). A better quantitative understanding of the mechanisms for N_2O production is crucial to develop novel strategies or new designs to mitigate N_2O.

The principle goal of this study was to investigate N_2O dynamics and determine N_2O production pathways in two intermittently-fed lab-scale sequencing batch reactors (SBRs) with high nitritation performance. This was achieved by N_2O online measurements and *in situ* applications of ^{15}N labeled NH_4^+ or NO_2^- followed by monitoring of ^{15}N labeled and unlabeled products. In addition, the nitritation performance was assessed during the ~300 days of operation.

2. Materials and methods

2.1. Setup and operation of sequencing batch reactors (SBRs)

2.1.1 Reactor description and operation

Two SBRs (R1 and R2) with a working volume of 5L were used (Fig. S1, Support information). Air supply was introduced by a bubble air diffuser and continuous mixing was provided with a magnetic stirrer during the reaction and feeding phase. Air supply, mixing, and actuation of pumps for fill and discharge were controlled by a programmable power strip EG-PM2-LAN (Gembird Software Ltd., Almere, Netherlands).

R1and R2 were operated as duplicates for 121 days, stopped for 170 days, where the biomass was stored separately at 4 °C, and restarted for another 172 days. The operation period can be divided into two phases: phase 1 (day 0−121) and phase 2 (day 291−463). The NH_4^+ and oxygen loading were the two manipulative variables to sustain a low NOB/AOB activity. To recover biomass activity after storage and maintain high NO_2^- accumulation, excess NH_4^+ and oxygen limitation were set by stepwise increasing the ammonium loading rate (ALR) and air flow rate from 0.29 to 0.79 g N/L/d and 0.2 to 0.55 L/min, respectively (Table S1).

A 6-h working cycle was applied over the entire experiment. One cycle consisted of 320 min reaction phase including five consecutive intervals of 1 minute feeding followed by a 63 minutes inter-feed period, 30 min settling phase, 5 min decanting phase and 5 min idle phase. The volumetric exchange ratio (VER) was 50%, resulting in a hydraulic retention time (HRT) of 12h. The sludge retention time (SRT) was controlled at 20 days by wasting sludge at the end of reaction phase. The reactors were operated at room temperature (20−26 °C) and without pH control.

2.1.2. Seed sludge and synthetic wastewater

The seeding sludge, originated from the return activated sludge stream at Mølleåværket WWTP (Lyngby, Denmark), was pre-cultivated and then inoculated into two SBRs.

Ammonium bicarbonate (NH_4HCO_3) was the only nitrogen source in the synthetic wastewater while NH_4HCO_3 and sodium bicarbonate ($NaHCO_3$) provided the inorganic carbon. The composition of trace chemicals (van de Graaf et al., 1996) was: 169.7 mg/L KH_2PO4, 751.1 mg/L $MgSO4{\cdot}7H_2O$, 451.6 mg/L $CaCl_2{\cdot}2H_2O$, 5 mg/L EDTA, 5 mg/L $FeSO_4{\cdot}7H_2O$ and trace element solution of 1mL/L. The trace element solution contained 0.43 mg/L $ZnSO_4{\cdot}7\ H_2O$, 0.24mg/L $CoCl_2{\cdot}6H_2O$, 0.99mg/L $MnCl_2{\cdot}4H_2O$, 0.25mg/L $CuSO_4{\cdot}5H_2O$, 0.22mg/L $NaMoO_4{\cdot}2H_2O$, 0.19mg/L $NiCl_2{\cdot}6H_2O$ and 0.21mg/L $NaSeO_4{\cdot}10H_2O$.

2.2. N_2O measurement

Liquid phase N_2O was analyzed by a N_2O-R Clark-type microsensor (UNISENSE A/S, Århus, Denmark) and data was logged every 30s. Off-gas N_2O concentration was measured during phase 2 and logged on a minute basis (Teledyne API, San Diego, USA) to compare liquid and off-gas N_2O dynamics. As the reactors were not completely gas-tight during the periodic off-gas N_2O measurements, the liquid phase N_2O concentrations were used for the quantification of N_2O emission rates.

Net N_2O production and emission rates were calculated from the following equations:

Instantaneous net N_2O production rate , $r_{N_2O_i} = \frac{\Delta N_2O_i}{\Delta t} + k_L a_{N_2O_i} \cdot N_2O_i$ Eq. 1

Daily averaged net N_2O production rate, $R_{N_2O} = \sum (r_{N_2O_i} \cdot \Delta t) \times 4 \frac{\text{cycle}}{\text{day}}$ Eq. 2

Where $r_{N_2O_i}$ is the instantaneous net N_2O production rate at time i, $\frac{\Delta N_2O_i}{\Delta t}$ is the differential term of liquid concentration at time i, and $k_L a_{N_2O_i} \cdot N_2O_i$ is the stripping rate at time i, which equals the

119 emission rate. The N_2O volumetric mass transfer coefficient ($k_L a_{N_2O}$) was determined
120 experimentally at different volume/flow rates scenarios (Domingo-Félez et al., 2014) (Table S2).
121 The net N_2O produced per NH_4^+oxidized ($\Delta N_2O/\Delta NH_4^+$, %) and the specific net N_2O production
122 rate (N_2OR, mg N/g VSS/d) were calculated from the daily averaged net N_2O production rate (Eq.
123 2).

124 **2.3. DNA extraction and qPCR**

125 Biomass samples were collected periodically from SBRs and centrifuged at 10,000 rpm for 5 min.
126 Pellets were stored at -80 °C until DNA extraction. DNA was extracted by FastDNA™ SPIN Kit
127 for Soil (MP Biomedicals, Solon, OH, USA), according to the manufacturer's instructions. The
128 quantity and quality of the extracted DNA was measured and checked by its 260/280 ratio with a
129 NanoDrop (ThermoFisher Scientific, Rockwood, TN, USA), and was stored at -20 °C until further
130 processing within a couple of weeks. qPCR was carried out on all the extracted DNA samples to
131 determine the relative abundance of ammonia-oxidizing bacteria (AOB), nitrite-oxidizing bacteria
132 (*Nitrobacter* NOB, *Nitrospira* NOB), anammox (AnAOB) and denitrifying bacteria, based on
133 appropriate 16S rRNA targets and functional genes. Details on the procedure can be found in
134 Terada et al. (2010). Primers and conditions used in various genes detection are listed in Table S3.
135 All samples, including control reactions without template DNAs, were measured in duplicates.

136 **2.4. ^{15}N additions and analysis**

137 A ^{15}N experiment was designed to identify the microbial sources of N_2O production during
138 operation of the nitritation SBRs (day 106 to 111). The ^{15}N-labeled nitrogen compounds (>98% ^{15}N;
139 Sigma-Aldrich) were added together with the second feed during the same cycle on different days
140 (Table S4).

The resulting ^{15}N mole fractions of the nitrogen pools was 17-18% for $^{15}NH_4^+$ and 11-13 % for $^{15}NO_2^-$, as determined from the isotopic ^{15}N and total concentrations after additions. Reactor liquid (12 ml) was sampled every 10 minutes after tracer additions until the fourth feed of the cycle. For isotopic analysis of N_2O and N_2, 3-mL and 6-ml Exetainer vials, respectively, prefilled with 100 µL of 50% (w/v) $ZnCl_2$ to stop microbial activity, were filled completely and immediately screw-capped with butyl rubber septa. Previous experiments had shown that $ZnCl_2$ efficiently quenched N transformations in this biomass (data not shown). The rest of the sample was filtered (0.22 µm) and frozen immediately for later analyses of nutrients and isotopic composition of NH_4^+, NO_2^- and nitrate (NO_3^-).

Just before isotopic analysis of N_2O and N_2, 1 and 1.5 ml of water was removed with a syringe and needle through the septum of the 3-mL and 6-mL Exetainer vials, respectively, while replacing the volumes with helium. The isotopic composition and concentration of N_2O and N_2 were determined using a gas chromatograph-isotope ratio mass spectrometer (Thermo Electron, Delta V advantage system) by injecting 1-mL and 200-µL samples of headspace directly from the Exetainer vials (Dalsgaard et al., 2012). The N-isotopic composition of NH_4^+ was analyzed after conversion to N_2 with hypobromite (Warembourg, 1993). $^{15}NO_2^-$ was converted to N_2 with sulfamic acid (Füssel et al., 2012), while $^{15}NO_3^-$ was analyzed, after removal of any $^{15}NO_2^-$ with sulfamic acid, by cadmium reduction followed by conversion of the NO_2^- product to N_2 with sulfamic acid (McIlvin and Altabet, 2005).

Rates of ^{15}N-labeled N_2O and N_2 production were calculated from the measured excess concentrations of $^{14}N^{15}NO$, $^{15}N^{15}NO$, $^{14}N^{15}N$, and $^{15}N^{15}N$ and the k_La for N_2O and N_2, respectively, similar to the calculations for bulk net N_2O production rate described above.

The total conversion of NH_4^+ and NO_2^- to the gaseous products, irrespective of the pathway, was determined by division of the rate of ^{15}N-labeled gas production ($^{15}N\text{-}N_2O = {}^{14}N^{15}NO + 2$ x

$^{15}N^{15}NO$; $^{15}N\text{-}N_2 = {}^{14}N^{15}N + 2 \times {}^{15}N^{15}N$) by the labeling fraction F of the substrate ($F_A = [{}^{15}NH_4^+] \times [NH_4^+]^{-1}$ and $F_N = [{}^{15}NO_2^-] \times [NO_2^-]^{-1}$), e.g.:

$$\text{Rate}(NH_4^+ \rightarrow N_2O) = \text{Rate}({}^{15}NH_4^+ \rightarrow {}^{15}N\text{-}N_2O) \times F_A^{-1} \quad \text{Eq. 3}$$

Production of N_2O through denitrification in the $^{15}NO_2^-$ experiments was calculated in two ways (Eq. 4 and 5), both based on the principle of random nitrogen isotope pairing (Nielsen, 1992) and resting on the assumption that denitrification is the only source of double-labeled products with $^{15}NO_2^-$. Here, Eq. 4 represents a rate based on NO_2^- in the bulk liquid only, with a known F_N, and Eq.5 represents a situation where F_N at the site of reaction may differ from that in the bulk liquid and is instead estimated from the ratio of $^{15}N^{15}NO$ production to $^{14}N^{15}NO$ production, R_{46}:

$$\text{Denitrification}_{N_2O,\ \text{bulk}} = \text{Rate}({}^{15}N\ {}^{15}NO) \times F_A^{-2} \quad \text{Eq. 4}$$

$$\text{Denitrification}_{N_2O,\ \text{coupled}} = \text{Rate}({}^{15}N\ {}^{15}NO) \times (2R_{46} \times [1+2R_{46}]^{-1})^{-2} \quad \text{Eq. 5}$$

2.5. Analytical methods

Liquid effluent samples were filtered through 0.45 μm pore size filters before nitrogen species analysis. NH_4^+ and NO_2^- were measured colorimetrically according to Bower and Holm-Hansen (1980) and Grasshoff (1999) respectively, while NO_3^- was analyzed by autoanalyzer (AutoAnalyzer 3, SEAL Analytical) with the cadmium-reduction method (Armstrong et al., 1967; Grasshoff, 1999). Reactor performance was described by computing the observed ammonium oxidizing rate (AOR, mg N/L/d), nitrite accumulation rate (NiAR, mg N/L/d), nitrate accumulation rate (NaAR, mg N/L/d) (Eq. S2-4). Free ammonia (FA) and free nitrous acid (FNA) concentration were calculated following Anthonisen et al. (1976) (Eq. S5-6). Mixed liquid suspended solids (MLSS) and mixed liquor volatile suspended solids (MLVSS) were measured following standard methods (APHA, 1998). DO and pH were monitored continuously (WTW GmbH, Weilheim, Germany).

3. Results

3.1. Reactor performance

3.1.1. Nitritation performance

Both reactors were operated towards high nitritation performance, and displayed stable NH_4^+ removal at the end of phase 1 (day 78–121) and phase 2 (day 291–463) (Fig. 1). At the loading of 0.57 g N/L/d at the end of phase 1, the average ammonium oxidizing efficiency (AOR/ALR) was 83 ± 12% (average ± standard deviation) and 90 ± 11% for R1 and R2, respectively. With stepwise increases in loading from 0.29 to 0.79 g N/L/d during phase 2, the average AOR/ALR remained relatively stable at 86 ± 11% (R1) and 88 ± 8% (R2) during phase 2, except for a ~19% decline in the final days of the reactors (Fig. 1). There was high NO_2^- accumulation at the end of phase 1 and throughout phase 2, maintaining average nitrite accumulation efficiency (NiAR/AOR) of 92 ± 17% and 93 ± 14% in R1 and R2, respectively. NO_3^- accumulated at low concentrations throughout the whole operation period (Fig. 1). Nitrate accumulation efficiency (NaAR/AOR) in R1 and R2 was maintained at 11 ± 9% and 14 ± 8% respectively, indicating low NOB activity.

3.1.2. In-cycle dynamics of nitrogen species, DO and pH

The reactors were operated with five intermittent feedings, without on-line pH control, and pH slightly decreased from 7.85 to 7.55 within a cycle (Fig. 2). pH transiently increased after each feeding due to the bicarbonate and phosphate content of the influent. During the inter-feed periods, pH decreased due to proton release during nitritation. DO concentrations were close to the limit of quantification of 0.1 mg/L during the reaction phase (Fig. 2). NH_4^+ concentration increased at each feeding while NO_2^- concentration decreased due to dilution. Concentrations of FA and FNA varied between 1.39 to 4.79 mg N/L and 0.005 to 0.013 mg N/L, respectively, reflecting the changes in NH_4^+ and NO_2^- concentrations at different pH (Fig. 2). During the inter-feed periods, AOR was relatively constant with an average value of 0.49 ± 0.04 mg N/L/min (Fig. 2).

3.2. N_2O production

3.2.1. Overall N_2O production

During the end of phase 1, the average net N_2O produced per NH_4^+ oxidized ($\Delta N_2O/\Delta NH_4^+$) in R1 and R2 was 0.6 ± 0.2% and 0.8 ± 0.3% respectively; while it was 2.0 ± 1.0% and 2.1 ± 0.7% during phase 2 (Table 1). The liquid N_2O concentrations as well as $\Delta N_2O/\Delta NH_4^+$ increased during phase 2 (Fig. 3 and Table 1) in two reactors. The differences in the specific net N_2O production rate (N_2OR) between the two reactors were likely due to the differences in MLVSS concentrations. Furthermore, each inter-feed period did not contribute equally to the total N_2O production of a cycle. N_2O gas escaping after feed 1, ranging between 23 to 41% in both reactors during two phases, was considerable higher compared to the emissions following the other feeds (Table 1).

3.2.2. N_2O dynamics during intermittent feedings

The patterns of liquid N_2O concentration profiles over the reaction phase were very reproducible during the whole period for both reactors (Fig. 2 and 3). In-cycle N_2O profiles had the following pattern: after the settling phase from the previous cycle, an initial maximum in N_2O concentration occurred when the first feed initiated, after which the concentration declined until the next feeding; another four smaller peaks in N_2O concentration were observed in the subsequent feedings. N_2O concentration reached minimum values in the inter-feed periods but with concentrations higher than the detection limit of the sensor. Thus, based on liquid N_2O concentrations there was always a positive net production of N_2O in both reactors, with rates ($r_{N_2O_i}$) increasing after each feeding and decreasing during inter-feed periods (Fig. 3). Off-gas N_2O profiles followed the same trends during the reaction phase.

3.3. Microbial community composition dynamics

The optimization of the reactor operation during phase 1 caused clear shifts in the microbial community, as indicated by qPCR analysis using relevant primers (Fig. 4). The microbial community composition was similar between the two reactors. The relative abundance of *Nitrobacter* spp. decreased at the end of phase 1, where *Nitrobacter* spp. was 2–3 orders of magnitude higher than *Nitrospira* spp. Both *Nitrobacter* spp. and *Nitrospira* spp remained very low throughout phase 2. Both 16S rRNA gene and *nxrA* targeted NOB quantifications were consistent in phase 2 (Fig. 4 and S2). The overall reduction in NOB relative abundance was mirrored by a significant increase in AOB numbers, as reflected by both the 16S rRNA gene and *amoA* targeted quantifications (Fig. 4 and S2). AOB remained dominant in both reactors throughout the operation period. The relative abundance of AnAOB, based on 16S rRNA gene quantification, was low but existent (0.96 ± 0.01% and 1.94 ± 0.01% in R1 and R2, respectively). The ratio of *nirS* plus *nirK* over *nosZ*-targeted quantifications was far above 1 (Fig. S2).

3.4. N_2O production pathway

In incubations with ^{15}N-labeled substrates, the label was transferred to both N_2O and N_2 within 2–3 minutes of addition, irrespective of whether ^{15}N was added as $^{15}NO_2^-$ or $^{15}NH_4^+$ (Fig. 5). The dynamics of ^{15}N-N_2O mirrored those of bulk N_2O, and N_2O was the dominating product in $^{15}NO_2^-$ incubations accounting for 57–58% of the labeled $N_2O + N_2$ in both feedings, while it only accounted for 17–23% with $^{15}NH_4^+$. The production of N_2 was also highly dynamic, showing an even steeper rise after feeding than for N_2O. The production of ^{15}N-N_2O from $^{15}NO_2^-$ corresponded to a total conversion of NO_2^- to N_2O of 5.7–9.9 µg N/g VSS/min, which was not significantly different from the total net N_2O production (Table 2), implying that NO_2^- was the main source of N_2O in the incubations.

255 There was no detectable production of $^{15}NH_4^+$ in the incubations with $^{15}NO_2^-$ (data not shown),
256 which implies that all ^{15}N-N_2O and ^{15}N-N_2 in these incubations was formed exclusively through
257 reductive pathways, i.e., not via dissimilatory nitrate/nitrite reduction to ammonium (DNRA) and
258 subsequent oxidation of NH_4^+.

259 Indeed, the relative production of $^{14}N^{15}NO$ and $^{15}N^{15}NO$ from $^{15}NO_2^-$ (Fig. 5) was close to that
260 expected from denitrification with random isotope pairing (either heterotrophic or nitrifier
261 denitrification). Thus, the production of N_2O through denitrification (calculated by Eq. 4)
262 corresponded to 80% and 77% of total net N_2O production from NO_2^- (the NO_2^--to-N_2O conversion
263 rates calculated by Eq. 3) on average for feed 2 and 3, respectively (Table 2). The remaining 20–
264 23% of NO_2^--derived N_2O corresponds to a surplus of $^{14}N^{15}NO$ relative to the prediction from
265 random isotope pairing from the bulk NO_2^- pool, and therefore indicates pairing of N from this pool
266 with N from a second source of unlabeled N. The surplus of $^{14}N^{15}NO$ may arise if the labeling
267 fraction of NO_2^-, F_N, in the immediate vicinity of the nitrite reductase enzymes is lower than the
268 bulk F_N value used for the calculations (Eq. 4), e.g., because of dilution with unlabeled NO_2^- from
269 nitritation maintained by diffusional gradients either intracellularly or within microaggregates. This
270 is reflected in the N_2O production calculated by Eq. 5, which derives F_N at the site of NO_2^-
271 reduction from the relative production of $^{14}N^{15}NO$ and $^{15}N^{15}NO$. Thus, assuming that all conversion
272 of NO_2^- to N_2O occurred through a denitrification pathway, total N_2O production was calculated
273 based on the relative production of $^{14}N^{15}NO$ and $^{15}N^{15}NO$ (Nielsen, 1992), yielding rates that
274 exceeded the NO_2^--to-N_2O conversion rates by 24–31% (Table 2).

275 The production of N_2O from NH_4^+, determined in incubations with $^{15}NH_4^+$ showed very similar
276 temporal dynamics as N_2O production from NO_2^- (Fig. 5). After the 2nd feed, the production from
277 NH_4^+ corresponded, on average, to 42% of the production from NO_2^- (Table 2). This fraction
278 increased to 58% after the 3rd feed, which is explained by the accumulation of $^{15}NO_2^-$ and the

resulting increasing contribution of $^{15}N_2O$ from denitrification, as also reflected in the higher concentrations of ^{15}N-N_2O reached after the 3rd feed relative to the 2nd (Fig. 5). The amount of ^{15}N-N_2O produced from $^{15}NH_4^+$ via nitritation, mixing of the formed $^{15}NO_2^-$ with the bulk NO_2^- pool, and subsequent denitrification, was estimated for each reactor based on the rates of N_2O production determined in the $^{15}NO_2^-$ incubations in the same reactor and the F_N values (data not shown) from the $^{15}NH_4^+$ incubations (Eq. 3). These calculations indicated that 25% and 49% of N_2O production determined with $^{15}NH_4^+$ occurred via bulk NO_2^- after feed 2 and 3, respectively. The $^{15}NH_4^+$-based N_2O production that was not attributable to this route averaged 2.6 µg N/g VSS/min after both feedings, corresponding to 25% of the combined N_2O production detected with $^{15}NO_2^-$ and $^{15}NH_4^+$ (Table 2), and the sum of this rate and the production of N_2O from NO_2^- matched the estimated N_2O production from denitrification closely (7.7 vs. 7.3 µg N/g VSS/min and 12.1 vs. 12.5 µg N/g VSS/min for R1 and R2, respectively). The contribution of the hydroxylamine oxidation pathway to N_2O production did *not* increase immediately after the addition of NH_4^+, as the production ratio between $^{15}N^{15}NO$ and $^{15}N^{14}NO$ did not change significantly over time after feed 2 and 3. Thus, the $^{15}NO_2^-$ and $^{15}NH_4^+$ in combination support a denitrification pathway as the main and possibly sole source of N_2O in this SBR system.

In the $^{15}NO_2^-$ incubations, the relative abundance of single and double-labeled N_2 ($^{14}N^{15}N$ and $^{15}N^{15}N$) differed markedly from that of N_2O, with $^{15}N^{15}N$ accounting for ≤0.5% of the labeled N_2 compared a contribution of ~5% from $^{15}N^{15}NO$ to labeled N_2O (Fig. 5). This pointed towards another N_2 source than denitrification. The total N_2 production rate from NO_2^- (Eq. 3) was 4.4 ± 0.9 and 6.4 ± 0.8 µg N/g VSS/min for R1 and R2, respectively. Substantially higher N_2 production rates were obtained for the $^{15}NH_4^+$ than with $^{15}NO_2^-$: 10.2 ± 3.5 and 21 ± 0.8 µg N/g VSS/min for R1 and R2, respectively. Correction of these rates for ^{15}N-N_2 produced from the accumulating $^{15}NO_2^-$

(performed similarly as for the N_2O production rates from $^{15}NH_4^+$) only reduced these rates slightly to 9.4 ± 3.5 and 19.7 ± 1.5 µg N/g VSS/min, respectively.

4. Discussion

4.1. Mechanisms to achieve high and stable nitritation performance

Two SBRs were operated for approximately 300 days with high NO_2^- accumulation and no significant production of NO_3^-, which indicates that NOB were successfully outcompeted by AOB (Fig. 1). The suppression of NOB and enrichment of AOB was verified by an average AOB/NOB ratio of >200 at the end of phase 1 and during phase 2 (Fig. 4). Various parameters such as DO, FA, FNA, temperature and feeding strategy have been reported to affect the selective enrichment of AOB over NOB (Blackburne et al., 2008; Hellinga et al., 1998; Liu and Wang, 2014; Vadivelu et al., 2007; Yang et al., 2013).

Oxygen limitation is a critical factor to achieve and maintain high nitritation performance. AOB are postulated to outcompete NOB at low DO concentrations due to the higher oxygen affinity of AOB than NOB (Blackburne et al., 2008; Wiesmann, 1994). DO below 1.0 mg/L was previously reported to inhibit the growth of NOB and instead enhance the growth of AOB, resulting nitrite accumulation (Sinha and Annachhatre, 2007; Tokutomi, 2004). For instance, stable nitrite accumulation efficiency (NiAR/AOR) of 70% and 85% is achieved at DO of 0.1 mg/L and 0.5–1.0 mg/L, respectively (Gao et al., 2016; Guo et al., 2013). As the DO level in our two nitritation SBRs was ≤ 0.1 mg/L, oxygen limitation is an important factor for NOB inhibition at the end of phase 1 and throughout phase 2, where high nitritation efficiencies of 92 ± 17% (R1) and 93 ± 14% (R2) were maintained (Fig. 1).

Among other factors, FA and FNA are commonly selected as the key parameters to achieve high nitritation because of the different impacts on AOB and NOB (Anthonisen et al., 1976; Brockmann and Morgenroth, 2010; Vadivelu et al., 2007; Yamamoto et al., 2008). Many studies have reported FA and FNA concentrations that might inhibit NOB growth and trigger AOB proliferation; however, the critical values reported in these studies were variable (Anthonisen et al., 1976; Bae et al., 2001; Vadivelu et al., 2007). Regarding FA, NOB has been found to be inhibited at concentrations ranging from 0.1 to 1 mg N/L, while AOB was inhibited at 10-150 mg N/L (Anthonisen et al., 1976). This agrees with a recent study by Vadivelu and coworkers (2007), where NOB activity was totally inhibited by 6.0 mg N/L and AOB activity was unaffected at up to 16 mg N/L. The increase in FA concentration by a factor of ~5 from phase 1 I to phase 1 II and 2, where the FA concentration was 3.1 ± 0.8 mg N/L, could be the reason for a decrease in nitrate accumulation, especially in R1 (Fig. 1 and 2). However, FA did not fully inhibit the activity of NOB at any time in our study. Also, within the observed FA concentration, FA likely had no effect on the activity of AOB.

It has been reported that NOB activity was inhibited by FNA at concentrations between 0.02 and 0.2 mg N/L (Hellinga et al., 1998; Vadivelu et al., 2007). Compared to these studies, FNA at 0.008 ± 0.002 mg NO_2^--N/L was too low to have a negative effect on NOB activity (Fig. 2). Throughout the whole SBR operation period, AOR correlated positively with NO_2^- concentrations, reaching the maximum (0.8 g N/L/d) at 323 mg N/L (Fig. S3). Hence, no evidence of NO_2^- inhibition was obtained. The observed increase in AOR with increasing NO_2^- concentration agrees with a previous study with mixed microbial communities, showing high ammonium oxidation to NO_2^- (150−160 mg NO_2^-N/h/g VSS) at NO_2^- concentrations up to 1000 mg N/L (Law et al., 2013). Nevertheless, the calculated FNA concentrations in this study (ca. 0.008 mg HNO_2^--N/L) remain much below reported inhibitor concentrations (FNA of 0.1 mg/L) (Hiatt and Grady, 2008).

Temperature is another parameter that can affect the relative competitiveness of AOB over NOB. NOB were outcompeted by AOB at moderate temperatures (20-26 °C), resulting in high nitritation efficiency from day 78 onwards (Fig. 1). This finding contrasts with the general assumption of high temperatures (30-35 °C) are needed for selective removal of NOB over AOB (Hellinga et al., 1998; Yang et al., 2007).

It is often difficult to maintain stable nitritation over the long-term period even in successfully established nitritation systems (Bernet et al., 2001; Fux et al., 2004; Villaverde et al., 2000; Yang et al., 2013). For instance, Villaverde and coworkers (2000) obtained high NiAR/AOR of 65% in submerged nitrifying biofilters, however, after 6 months NOB became acclimated to high FA and NiAR/AOR decreased to 30%. Moreover, Bernet and coworkers (2001) observed a transition from stable nitritation in a two-stage PN-anammox process for more than 100 days to complete nitrification within 2 days caused by a transient increase of DO. Here, SBRs were operated for ~300 days with high nitritation efficiency and high AOB abundance accompanied by low NO_3^- accumulation and low NOB abundance. We speculate that using intermittent feeding together with low DO set-points successfully enabled long-term high nitritation performance in the two SBR reactors. While long-term high-rate nitritation has not been reported yet in intermittently fed SBRs, high nitrite accumulation (NiAR/AOR) of 85% and >95% was previously reported for 150 and 174 days, respectively, in step-feed A/O SBRs (Lemaire et al., 2008; Yang et al., 2007). Hence, low DO control and intermittent feeding appear key operational strategies to obtain continuous NOB suppression at suboptimal temperatures.

4.2. Low N_2O production

The net N_2O produced per NH_4^+ oxidized ($\Delta N_2O/\Delta NH_4^+$) and the specific net N_2O production rate (N_2OR) of the two nitritation SBRs were compared to previously reported values together with the identification of reactor types, operation strategies, performance and AOB presence (Table S5). The

372 average net N_2O production in phase 2 increased to 2.0 ± 1.0% and 2.1 ± 0.7% of the NH_4^+ oxidized
373 in R1 and R2, respectively, while the average specific net N_2O production rate was 8.4 ± 3.5 and
374 10.2 ± 3.5 mg N/g VSS/d in R1 and R2, respectively (Table 1 and S5). The net N_2O production in
375 both reactors corresponded well with the genetic potential for N_2O production, as the ratio of *nirS*
376 plus *nirK* over *nosZ*-targeted genes was far above 1 (Fig. S2). The higher N_2O production in phase
377 2 compared to phase 1 is puzzling as it cannot be explained by higher AOR (Table 1). We speculate
378 that the long-term operation under elevated NO_2^- may have selected for new microbes with higher
379 expression of the nitrifier-denitrification pathway or the cultured microbes adapted to higher NO_2^-,
380 resulting in higher expression of the pathway, and with that higher N_2O production. This theory,
381 however, calls for deeper analysis of the microbial community than obtained with qPCR.

382 The N_2O production factors of ~2% are in the low range of previous reports for both lab-scale and
383 full-scale PN systems, ranging between 1–17% (Table S5). Our study is the first study to measure
384 low N_2O emissions at very high nitritation efficiencies. Low DO (0.35 mg/L) and high NO_2^-
385 conditions (10 – 50 mg N/L) boost N_2O production (Peng et al., 2015, 2014). Measured N_2O
386 emissions are lower compared to other lab-scale PN SBRs operated under low DO and high NO_2^-
387 conditions (N_2O emissions of 17%) (Gao et al., 2016; Lv et al., 2016). With the intermittent feeding
388 strategy at low DO, we force relatively low ammonia oxidation rates (Fig. 2, Table 1), which has
389 previously been shown to decrease N_2O emissions from autotrophic nitrogen removal systems
390 (Domingo-Félez et al., 2014; Law et al., 2011). Law and coworkers (2011) found that a decline in
391 feeding rate from 1 L/2.5 min to 1 L/25 min during the reaction phase lead to a substantial reduction
392 in N_2O production without affecting the nitritation performance. Instead of reducing the feeding rate,
393 our nitritation reactors were operated with five intermittent feedings within a cycle. This step-feed
394 strategy has previously been suggested as an effective optimization approach to reduce N_2O

emissions from SBRs (Mavrovas, 2014; Yang et al., 2009, 2013). Therefore, we postulate that intermittent feeding is the cause for the low N_2O emission from high-performance nitritation system.

4.3. Potential pH effect on in-cycle N_2O production dynamics

Distinctive N_2O production profiles were observed within the representative cycles (Fig. 2 and 3). The maximum net N_2O production and the subsequent decrease after the first feed has also been described in various studies (Ali et al., 2016; Itokawa et al., 2001; Kampschreur et al., 2008; Mampaey et al., 2016; Rodriguez-Caballero and Pijuan, 2013). Rodriguez-Caballero and Pijuan (2013) showed that 60% of the total N_2O production occurred during the settling phase in their lab-scale PN SBR, while 70% of the quantified N_2O emission was attributed to the anoxic N_2O formation in a full-scale PN SHARON reactor (Mampaey et al., 2016). Tentative liquid N_2O measurements indicated that N_2O accumulated during the non-aerated settling phase (data not shown). Denitrification might be responsible for this N_2O accumulation during the settling phase, which is then released at the onset of aeration (Itokawa et al., 2001). The genetic potential for N_2O production by denitrifiers was present through the high relative abundance of *nirS* (Fig. S2).

A potential effect of pH on N_2O production during the reaction phase was indicated by the transiently increase in net N_2O production rates with the rise in pH after each feeding pulse (Fig. 2 and 3). There was no obvious changes in DO, and although NH_4^+ and FA increased transiently after each feeding, FA was always in excess compared to the K_m value of 0.0075 mg/L for AOB, and therefore AOR remained unaffected (Fig. 2) (Hiatt and Grady, 2008). Thus, pH appears the only potential variable affecting in-cycle N_2O dynamics. Only few studies have been able to isolate the effect of pH on N_2O production from the variations in FA and FNA, and the reported effect of pH on N_2O production differ. In contrast to our results, Law and coworkers (2011) obtained highest N_2OR and AOR at pH 8 in the investigated pH range of 6.0–8.5, independently from FA and FNA concentrations, suggesting that an increase in ammonium oxidation activity might promote N_2O

production. Oppositely, Rathnayake et al. (2015) observed highest N_2O emission at pH 7.5 in PN granules, although AOR was unchanged between pH 6.5 and 8.5. Further research is needed to resolve whether the pH effect on N_2O production is direct or indirect.

4.4. N_2O production pathway

The experiments with ^{15}N labeled substrates point to nitrifier denitrification as the dominant source of N_2O in the SBR nitritation systems. A denitrification-type process rather than a direct production of N_2O from ammonium oxidation via hydroxylamine was demonstrated by more than 3 times higher rates of N_2O production from NO_2^- than from NH_4^+, when $^{15}NH_4^+$-derived rates were corrected for accumulation of $^{15}NO_2^-$ (Table 2). Moreover, isotope pairing calculations showed that NO_2^- during its reduction to N_2O was mixed with nitrogen from an unlabeled source. In the nitritation-dominated system, NH_4^+ is the most obvious candidate, and indeed, the production rate of N_2O from NH_4^+ that did not go via bulk NO_2^- closely matched the difference between total and bulk NO_2^--dependent denitrification. We therefore hypothesize that essentially all N_2O was produced through nitrifier-denitrification with part of the newly-formed NO_2^- shunted directly to reduction either intracellullarly or within cellular aggregates before it could mix completely with NO_2^- in the bulk liquid. Alternatively, the combination of N from NH_4^+ and NO_2^- could occur at the level of NO if this compound is a free intermediate during ammonium oxidation (Stein, 2011). The ^{15}N-labeling technique in itself cannot distinguish nitrifier denitrification from heterotrophic denitrification. However, several pieces of evidence point to the former process. Firstly, the stimulation of N_2O production by each NH_4^+ feeding points to NH_4^+ dependence rather than heterotrophy. Secondly, there is no convincing evidence for heterotrophic N_2 production: (a) The rate of N_2O production exceeds the rate of N_2 production from NO_2^- whereas N_2O is generally a minor byproduct of heterotrophic denitrification (Betlach and Tiedje, 1981); (b) the dynamics of N_2 and N_2O production are out of phase with the peak in N_2 preceding that of N_2O, where the opposite

443 would be expected during heterotrophic denitrification (e.g., Jensen et al., 2009), and (c) the very
444 low ratio of $^{15}N^{15}N$ to $^{14}N^{15}N$, differing markedly from the $^{15}N^{15}NO$:$^{14}N^{15}NO$ ratio in N_2O, suggests
445 that N_2 production from NO_2^- is mainly due to another process, possibly anammox.

446 The complete dominance of nitrifier-denitrification as source of N_2O is in general agreement with
447 the understanding that this process is favored by low DO and high NO_2^- levels (e.g., Colliver and
448 Stephenson, 2000; Kampschreur et al., 2008; Peng et al., 2015; Tallec et al., 2006). The high rates
449 of N_2 production observed in the $^{15}NH_4^+$ incubations, relative to both N_2O production in the same
450 experiment and to N_2 production with $^{15}NO_2^-$, suggests an involvement of anammox. Only a small
451 part of the N_2 produced with $^{15}NH_4^+$ could be explained with oxidation to NO_2^- and subsequent
452 reduction, which means that NH_4^+ appeared to be converted directly from NH_4^+ to N_2. As N_2
453 production has not been documented in aerobic ammonium oxidizers, this suggests the involvement
454 of anammox bacteria, which were indeed detected in the biomass (Fig. 4) in low abundance. As
455 anammox represents a 1:1 pairing of N from NH_4^+ and NO_2^-, similar rates of N_2 production should,
456 however, be obtained with additions of $^{15}NH_4^+$ and $^{15}NO_2^-$ (van de Graaf et al., 1995), whereas we
457 observed ~2.5-fold higher production from $^{15}NH_4^+$ than from $^{15}NO_2^-$. Potential explanations for the
458 imbalance in rates are either a close coupling of nitritation and anammox, which would require a
459 physical association of anammox bacteria and ammonium oxidizers, or variation in anammox rates
460 between the two series of experiments, which were conducted 5 days apart. The resolution of these
461 issues is, however, beyond the scope of this study.

462 ## 5. Conclusion

463 Two lab-scale intermittently-fed nitritation SBRs were operated to investigate N_2O dynamics and
464 identify N_2O production pathways.

- High nitritation performance with ~93 ± 14% of the oxidized NH_4^+ converted to NO_2^- was achieved in intermittently-fed SBRs at 20-26℃ for ~300 days.
- The averaged net N_2O production factor of 2.1 ± 0.7% is in the low range: Operation with intermittent feeding may be an effective approach to minimize N_2O emissions from nitritation systems.
- Increased net N_2O production rate was observed with pH increase after each feeding. Further investigations are required to identify the exact mechanisms of the pH effect on enzymes, pathways and bacteria involved in N_2O production.
- Nitrifier denitrification was the dominant source of N_2O.

This study has demonstrated operational conditions (low dissolved oxygen and intermittent feeding) that achieve high-rate and long-term nitritation under normal temperature, which could enlarge the applicability of the nitritation process in WWTPs. The relatively low N_2O production at high nitritation efficiencies reduces the growing concern of N_2O production from autotrophic nitrogen processes in WWTPs. The identification of nitrifier denitrification as the main pathway of N_2O emissions will open up for more focused strategies to lower the N_2O footprint even more in nitritation systems.

Acknowledgements

The work has been funded in part by the China Scholarship Council, the Innovation Fund Denmark (IFD) (Project LaGas, File No. 0603-00523B) and The Danish Council for Independent Research Technology and Production Sciences (FTP) (Project N_2Oman, File No. 1335-00100B). The authors thank Lene Kirstejn Jensen for the assistance during qPCR measurements.

References

Ali, M., Rathnayake, R.M.L.D., Zhang, L., Ishii, S., Kindaichi, T., Satoh, H., Toyoda, S., Yoshida, N., Okabe, S., 2016.

Source identification of nitrous oxide emission pathways from a single-stage nitritation-anammox granular reactor. Water Res. 102, 147–157.

Anthonisen, A., Loehr, R., Prakasam, T., Srinath, E., 1976. Inhibition of Nitrification by Ammonia and Nitrous Acid. J. Water Pollut. Control Fed. 48, 835–852.

APHA, 1998. Standard Methods for the Examination of Water and Wastewater, 20th ed. American Public Health Association, Washington, DC.

Armstrong, F.A.J., Stearns, C.R., Strickland, J.D.H., 1967. The measurement of upwelling and subsequent biological process by means of the Technicon Autoanalyzer® and associated equipment. Deep Sea Res. Oceanogr. Abstr. 14, 381–389.

Bae, W., Baek, S., Chung, J., Lee, Y., 2001. Optimal operational factors for nitrite accumulation in batch reactors. Biodegradation 12, 359–66.

Bernet, N., Dangcong, P., Delgenès, J.-P., Moletta, R., 2001. Nitrification at Low Oxygen Concentration in Biofilm Reactor. J. Environ. Eng. 127, 266–271.

Betlach, M.R., Tiedje, J.M., 1981. Kinetic explanation for accumulation of nitrite, nitric oxide, and nitrous oxide during bacterial denitrification. Appl. Environ. Microbiol. 42, 1074–1084.

Blackburne, R., Yuan, Z., Keller, J., 2008. Partial nitrification to nitrite using low dissolved oxygen concentration as the main selection factor. Biodegradation 19, 303–312.

Bower, C.E., Holm-Hansen, T., 1980. A Salicylate–Hypochlorite Method for Determining Ammonia in Seawater. Can. J. Fish. Aquat. Sci. 37, 794–798.

Brockmann, D., Morgenroth, E., 2010. Evaluating operating conditions for outcompeting nitrite oxidizers and maintaining partial nitrification in biofilm systems using biofilm modeling and Monte Carlo filtering. Water Res. 44, 1995–2009.

Burgess, J.E., Colliver, B.B., Stuetz, R.M., Stephenson, T., 2002. Dinitrogen oxide production by a mixed culture of nitrifying bacteria during ammonia shock loading and aeration failure. J. Ind. Microbiol. Biotechnol. 29, 309–313.

Colliver, B.B., Stephenson, T., 2000. Production of nitrogen oxide and dinitrogen oxide by autotrophic nitrifiers. Biotechnol. Adv. 18, 219–232.

Dalsgaard, T., Thamdrup, B., Farías, L., Revsbech, N.P., 2012. Anammox and denitrification in the oxygen minimum zone of the eastern South Pacific. Limnol. Oceanogr. 57, 1331–1346.

Desloover, J., De Clippeleir, H., Boeckx, P., Du Laing, G., Colsen, J., Verstraete, W., Vlaeminck, S.E., 2011. Floc-based sequential partial nitritation and anammox at full scale with contrasting N2O emissions. Water Res. 45, 2811–2821.

Domingo-Félez, C., Mutlu, A.G., Jensen, M.M., Smets, B.F., 2014. Aeration strategies to mitigate nitrous oxide emissions from single-stage nitritation/anammox reactors. Environ. Sci. Technol. 48, 8679–8687.

Domingo-Félez, C., Pellicer-Nàcher, C., Petersen, M.S., Jensen, M.M., Plósz, B.G., Smets, B.F., 2017. Heterotrophs are key contributors to nitrous oxide production in activated sludge under low C-to-N ratios during nitrification-Batch experiments and modeling. Biotechnol. Bioeng. 114, 132–140.

Fux, C., Huang, D., Monti, A., Siegrist, H., 2004. Difficulties in maintaining long-term partial nitritation of ammonium-rich sludge digester liquids in a moving-bed biofilm reactor (MBBR). Water Sci. Technol. 49, 53–60.

Füssel, J., Lam, P., Lavik, G., Jensen, M.M., Holtappels, M., Günter, M., Kuypers, M.M., 2012. Nitrite oxidation in the

527 Namibian oxygen minimum zone. ISME J. 6, 1200–1209.
528 Gao, K., Zhao, J., Ge, G., Ding, X., Wang, S., Li, X., Yu, Y., 2016. Effect of Ammonium Concentration on N2O
529 Emission During Autotrophic Nitritation Under Oxygen-Limited Conditions. Environ. Eng. Sci. 0, 1–7.
530 Grasshoff, K., 1999. Methods of Seawater Analysis, 3rd ed. Wiley-VCH Verlag GmbH, Weinheim.
531 Guo, J., Peng, Y., Yang, X., Gao, C., Wang, S., 2013. Combination process of limited filamentous bulking and nitrogen
532 removal via nitrite for enhancing nitrogen removal and reducing aeration requirements. Chemosphere 91, 68–75.
533 Hellinga, C., Schellen, A.A.J.C., Mulder, J.W., Van Loosdrecht, M.C.M., Heijnen, J.J., 1998. The SHARON process:
534 An innovative method for nitrogen removal from ammonium-rich waste water. Water Sci. Technol. 37, 135–142.
535 Hiatt, W.C., Grady, C.P.L., 2008. An Updated Process Model for Carbon Oxidation, Nitrification, and Denitrification.
536 Water Environ. Res. 80, 2145–2156.
537 IPCC, 2013. Climate Change 2013: The Physical Science Basis, Cambridge University Press. Cambridge, United
538 Kingdom and New York, NY, USA.
539 Ishii, S., Song, Y., Rathnayake, L., Tumendelger, A., Satoh, H., Toyoda, S., Yoshida, N., Okabe, S., 2014.
540 Identification of key nitrous oxide production pathways in aerobic partial nitrifying granules. Environ. Microbiol.
541 16, 3168–3180.
542 Itokawa, H., Hanaki, K., Matsuo, T., 2001. Nitrous oxide production in high-loading biological nitrogen removal
543 process under low COD/N ratio condition. Water Res. 35, 657–664.
544 Jensen, M.M., Petersen, J., Dalsgaard, T., Thamdrup, B., 2009. Pathways, rates, and regulation of N2 production in the
545 chemocline of an anoxic basin, Mariager Fjord, Denmark. Mar. Chem. 113, 102–113.
546 Kampschreur, M.J., Tan, N.C.G., Kleerebezem, R., Picioreanu, C., Jetten, M.S.M., Van Loosdrecht, M.C.M., 2008.
547 Effect of dynamic process conditions on nitrogen oxides emission from a nitrifying culture. Environ. Sci. Technol.
548 42, 429–435.
549 Kartal, B., Kuenen, J.G., van Loosdrecht, M.C.M., 2010. Sewage Treatment with Anammox. Science (80-.). 328, 702–
550 703.
551 Kim, S.W., Miyahara, M., Fushinobu, S., Wakagi, T., Shoun, H., 2010. Nitrous oxide emission from nitrifying activated
552 sludge dependent on denitrification by ammonia-oxidizing bacteria. Bioresour. Technol. 101, 3958–3963.
553 Kong, Q., Liang, S., Zhang, J., Xie, H., Miao, M., Tian, L., 2013. N2O emission in a partial nitrification system:
554 Dynamic emission characteristics and the ammonium-oxidizing bacteria community. Bioresour. Technol. 127,
555 400–406.
556 Law, Y., Lant, P., Yuan, Z., 2013. The confounding effect of nitrite on N2O production by an enriched ammonia-
557 oxidizing culture. Environ. Sci. Technol. 47, 7186–7194.
558 Law, Y., Lant, P., Yuan, Z., 2011. The effect of pH on N2O production under aerobic conditions in a partial nitritation
559 system. Water Res. 45, 5934–5944.
560 Law, Y., Ye, L., Pan, Y., Yuan, Z., 2012. Nitrous oxide emissions from wastewater treatment processes. Philos. Trans.
561 R. Soc. B Biol. Sci. 367, 1265–1277.
562 Lemaire, R., Marcelino, M., Yuan, Z., 2008. Achieving the nitrite pathway using aeration phase length control and step-
563 feed in an SBR removing nutrients from abattoir wastewater. Biotechnol. Bioeng. 100, 1228–1236.
564 Liu, G., Wang, J., 2014. Role of Solids Retention Time on Complete Nitrification: Mechanistic Understanding and
565 Modeling. J. Environ. Eng. 140, 48–56.

566 Lv, Y., Ju, K., Wang, L., Chen, X., Miao, R., Zhang, X., 2016. Effect of pH on nitrous oxide production and emissions
567 from a partial nitritation reactor under oxygen-limited conditions. Process Biochem. 51, 765–771.
568 Mampaey, K.E., De Kreuk, M.K., van Dongen, U.G.J.M., van Loosdrecht, M.C.M., Volcke, E.I.P., 2016. Identifying
569 N2O formation and emissions from a full-scale partial nitritation reactor. Water Res. 88, 575–585.
570 Mavrovas, I., 2014. "GraNiti SBR" Start-up and Operation of a Granular Nitritatiing Sequencing Batch Reactor.
571 Technical University of Denmark.
572 McIlvin, M.R., Altabet, M.A., 2005. Chemical conversion of nitrate and nitrite to nitrous oxide for nitrogen and oxygen
573 isotopic analysis in freshwater and seawater. Anal Chem 77, 5589–5595.
574 Nielsen, L., 1992. Denitrification in sediment deermined from nitrogen isotope pairing technique. FEMS Microbiol.
575 Lett. 86, 357–362.
576 Peng, L., Ni, B.-J., Ye, L., Yuan, Z., 2015. The combined effect of dissolved oxygen and nitrite on N2O production by
577 ammonia oxidizing bacteria in an enriched nitrifying sludge. Water Res. 73, 29–36.
578 Peng, L., Ni, B.J., Erler, D., Ye, L., Yuan, Z., 2014. The effect of dissolved oxygen on N2O production by ammonia-
579 oxidizing bacteria in an enriched nitrifying sludge. Water Res. 66, 12–21.
580 Poughon, L., Dussap, C.-G., Gros, J.-B., 2001. Energy model and metabolic flux analysis for autotrophic nitrifiers.
581 Biotechnol. Bioeng. 72, 416–433.
582 Rathnayake, R.M.L.D., Oshiki, M., Ishii, S., Segawa, T., Satoh, H., Okabe, S., 2015. Effects of dissolved oxygen and
583 pH on nitrous oxide production rates in autotrophic partial nitrification granules. Bioresour. Technol. 197, 15–22.
584 Rodriguez-Caballero, A., Pijuan, M., 2013. N2O and NO emissions from a partial nitrification sequencing batch reactor:
585 Exploring dynamics, sources and minimization mechanisms. Water Res. 47, 3131–3140.
586 Schneider, Y., Beier, M., Rosenwinkel, K.-H., 2014. Influence of operating conditions on nitrous oxide formation
587 during nitritation and nitrification. Environ. Sci. Pollut. Res. Int. 21, 12099–12108.
588 Siegrist, H., Salzgeber, D., Eugster, J., Joss, A., 2008. Anammox brings WWTP closer to energy autarky due to
589 increased biogas production and reduced aeration energy for N-removal. Water Sci. Technol. 57, 383.
590 Sinha, B., Annachhatre, A., 2007. Assessment of partial nitrification reactor performance through microbial population
591 shift using quinone profile, FISH and SEM. Bioresour. Technol. 98, 3602–3610.
592 Stein, L.Y., 2011. Surveying N2O-Producing Pathways in Bacteria. Methods Enzymol. 486, 131–152.
593 Strokal, M., Kroeze, C., 2014. Nitrous oxide (N2O) emissions from human waste in 1970-2050. Curr. Opin. Environ.
594 Sustain. 9–10, 108–121.
595 Tallec, G., Garnier, J., Billen, G., Gousailles, M., 2006. Nitrous oxide emissions from secondary activated sludge in
596 nitrifying conditions of urban wastewater treatment plants: Effect of oxygenation level. Water Res. 40, 2972–
597 2980.
598 Terada, A., Lackner, S., Kristensen, K., Smets, B.F., 2010. Inoculum effects on community composition and nitritation
599 performance of autotrophic nitrifying biofilm reactors with counter-diffusion geometry. Environ. Microbiol. 12,
600 2858–2872.
601 Terada, A., Sugawara, S., Hojo, K., Takeuchi, Y., Riya, S., Harper, W.F., Yamamoto, T., Kuroiwa, M., Isobe, K.,
602 Katsuyama, C., Suwa, Y., Koba, K., Hosomi, M., 2017. Hybrid Nitrous Oxide Production from a Partial
603 Nitrifying Bioreactor: Hydroxylamine Interactions with Nitrite. Environ. Sci. Technol. 51, 2748–2756.
604 Tokutomi, T., 2004. Operation of a nitrite-type airlift reactor at low DO concentration. Water Sci. Technol. 49, 81–88.

605 Vadivelu, V.M., Keller, J., Yuan, Z., 2007. Free ammonia and free nitrous acid inhibition on the anabolic and catabolic
606 processes of Nitrosomonas and Nitrobacter. Water Sci. Technol. 56, 89–97.
607 van de Graaf, A.A., Bruijn, P. de, Robertson, L.A., Jetten, M.S.M., Kuenen, J.G., 1996. Autotrophic growth of
608 anaerobic ammonium-oxidizing micro-organisms in a fluidized bed reactor. Microbiology 142, 2187–2196.
609 van de Graaf, A.A. van de, Mulder, A., Bruijn, P. de, Jetten, M.S.M., Robertson, L.A., Kuenen, J.G., 1995. Anaerobic
610 oxidation of ammonium is a biologically mediated process. Appl. Environ. Microbiol. 61, 1246–1251.
611 Villaverde, S., Fdz-Polanco, F., García, P.A., 2000. Nitrifying biofilm acclimation to free ammonia in submerged
612 biofilters. Start-up influence. Water Res. 34, 602–610.
613 Wang, X.-H., Jiang, L.-X., Shi, Y.-J., Gao, M.-M., Yang, S., Wang, S.-G., 2012. Effects of step-feed on granulation
614 processes and nitrogen removal performances of partial nitrifying granules. Bioresour. Technol. 123, 375–381.
615 Warembourg, F.R., 1993. Nitrogen Fixation in Soil and Plant Systems, in: Knowles, R., Henry, B. (Eds.), Nitrogen
616 Isotope Techniques. Academic Press, New York, pp. 127–155.
617 Wett, B., Omari, A., Podmirseg, S.M., Han, M., Akintayo, O., Gómez Brandón, M., Murthy, S., Bott, C., Hell, M.,
618 Takács, I., Nyhuis, G., O'Shaughnessy, M., 2013. Going for mainstream deammonification from bench to full
619 scale for maximized resource efficiency. Water Sci. Technol. 68, 283.
620 Wiesmann, U., 1994. Biological nitrogen removal from wastewater. Adv. Biochem. Eng. Biotechnol. 51, 113–154.
621 Wrage, N., Velthof, G.L., Van Beusichem, M.L., Oenema, O., 2001. Role of nitrifier denitrification in the production of
622 nitrous oxide. Soil Biol. Biochem. 33, 1723–1732.
623 Yamamoto, T., Takaki, K., Koyama, T., Furukawa, K., 2008. Long-term stability of partial nitritation of swine
624 wastewater digester liquor and its subsequent treatment by Anammox. Bioresour. Technol. 99, 6419–6425.
625 Yang, Q., Liu, X., Peng, C., Wang, S., Sun, H., Peng, Y., 2009. N2O production during nitrogen removal via nitrite
626 from domestic wastewater: Main sources and control method. Environ. Sci. Technol. 43, 9400–9406.
627 Yang, Q., Peng, Y., Liu, X., Zeng, W., Mino, T., Satoh, H., 2007. Nitrogen Removal via Nitrite from Municipal
628 Wastewater at Low Temperatures using Real-Time Control to Optimize Nitrifying Communities. Environ. Sci.
629 Technol. 41, 8159–8164.
630 Yang, S., Gao, M.M., Liang, S., Wang, S.G., Wang, X.H., 2013. Effects of step-feed on long-term performances and
631 N2O emissions of partial nitrifying granules. Bioresour. Technol. 143, 682–685.
632

Table 1. Overview of AOR, N_2OR and $\Delta N_2O/\Delta NH_4^+$ in R1 and R2 during phase 1 and 2. The net N_2O produced during each feed is stated as the percentage of total net N_2O production during the entire cycle.

	R1		R2	
	Phase 1 (Day 106–112)	Phase 2 (Day 395–451)	Phase 1 (Day 106–112)	Phase 2 (Day 397–463)
AOR (g N/L/d)	0.5 ± 0.05	0.60 ± 0.05	0.5 ± 0.02	0.76 ± 0.06
AOR (g N/g VSS/d)	1.04 ± 0.11	0.46 ± 0.09	1.78 ± 0.08	0.5 ± 0.02
N_2OR (mg N/g VSS/d)	5.9 ± 1.8	8.4 ± 3.5	16.0 ± 5.9	10.2 ± 3.5
$\Delta N_2O/\Delta NH_4^+$(%)	0.6 ± 0.2	2.0 ± 1.0	0.8 ± 0.3	2.1 ± 0.7
Feed 1 (%)	23 ± 5	41 ± 9	30 ± 5	27 ± 5
Feed 2 (%)	22 ± 1	14 ± 2	21 ± 2	17 ± 2
Feed 3 (%)	19 ± 1	15 ± 2	18 ± 2	18 ± 2
Feed 4 (%)	17 ± 2	16 ± 2	16 ± 2	19 ± 1
Feed 5 (%)	18 ± 3	15 ± 4	15 ± 2	21 ± 5
# cycles	n=22	n=23	n=22	n=20

Table 2. Summary of net N_2O production rates during the ^{15}N experiment (µg N/g VSS/min). Bulk N_2O production was based on liquid N_2O concentrations, measured with microsensors, while N_2O source partitioning is based on isotope additions

	R1				R2			
	$^{15}NO_2^-$ additions				$^{15}NO_2^-$ additions			
Days of operation	110		111		110		111	
	Feed 2	Feed 3	Feed 2	Feed 3	Feed 2	Feed 3	Feed 2	Feed 3
Bulk N_2O production rate	4.7	4.7	6.9	7.1	12	13	10	9.3
N_2O production rate from NO_2^- (Eq. 3)	5.7	6.9	6.8	5.8	9.4	8.1	9.9	8.7
N_2O production from bulk NO_2^- through ND (Eq. 4)	4.9	6.2	6.2	4.6	6.6	5.1	7.3	6.5
Total N_2O production through ND (Eq. 5)	6.7	7.6	7.4	7.4	13	13	13	11
	$^{15}NH_4^+$ additions				$^{15}NH_4^+$ additions			
Days of operation	106		107		106		107	
	Feed 2	Feed 3	Feed 2	Feed 3	Feed 2	Feed 3	Feed 2	Feed 3
Bulk N_2O production rate	6.1	5.0	5.5	5.3	13	14	11	13
N_2O production from NH_4^+ (Eq. 3)	2.1	3.6	1.9	3.1	5.2	6.7	4.9	6.4
N_2O production via bulk NO_2^-	0.49	1.8	0.70	1.8	0.82	2.4	1.5	3.4
N_2O production not via bulk NO_2^-	1.6	1.8	1.2	1.3	4.4	4.3	3.4	3.0

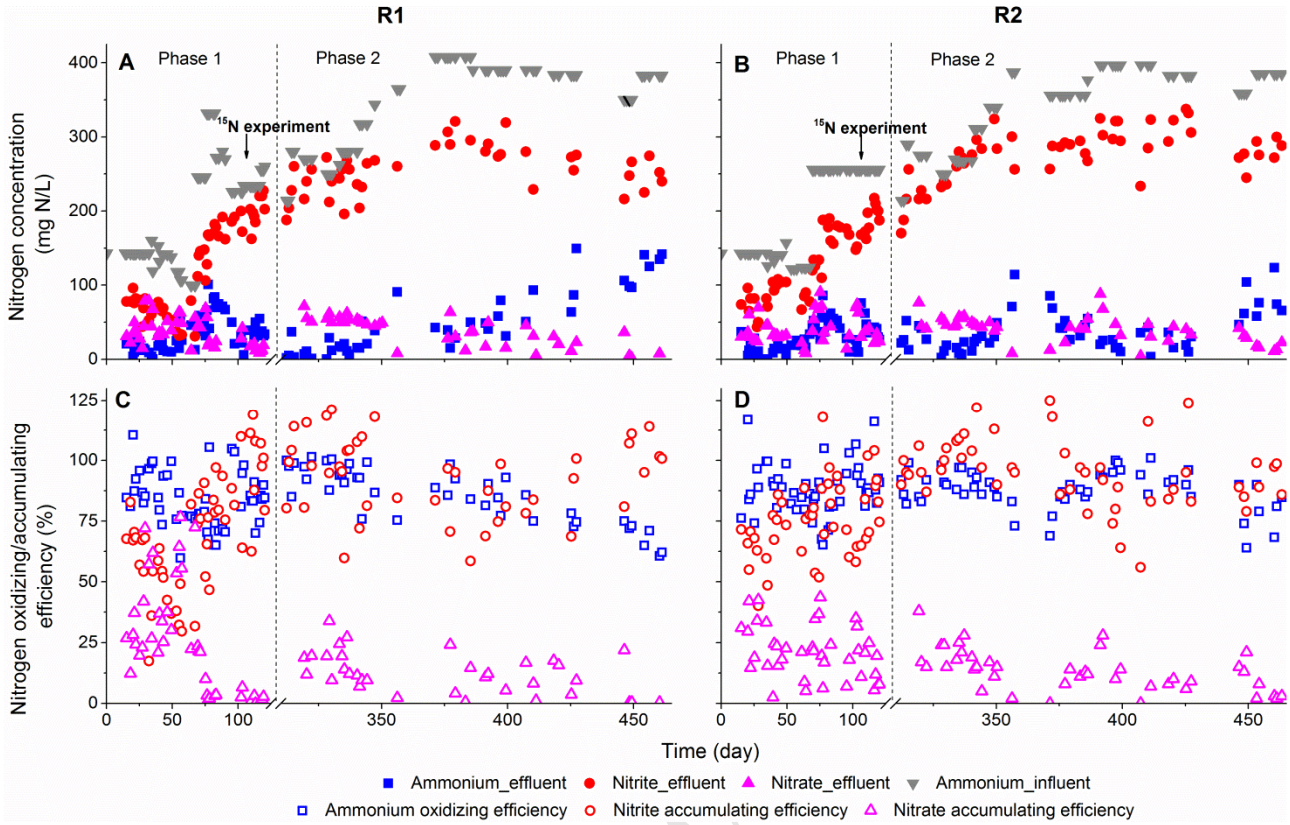

Fig. 1. Nitritation performance in R1 (A, C) and R2 (B, D) throughout the operational period. (A, B) Nitrogen concentrations (ammonium, nitrite and nitrate in effluent, ammonium in influent). (C, D) Nitrogen conversion efficiency (ammonium oxidizing efficiency (AOR/ALR), nitrite accumulation efficiency (NiAR/AOR), nitrate accumulation efficiency (NaAR/AOR)). The break at the X-axis represents a period of 170 days, when the reactors were stopped and biomass was stored at 4 °C.

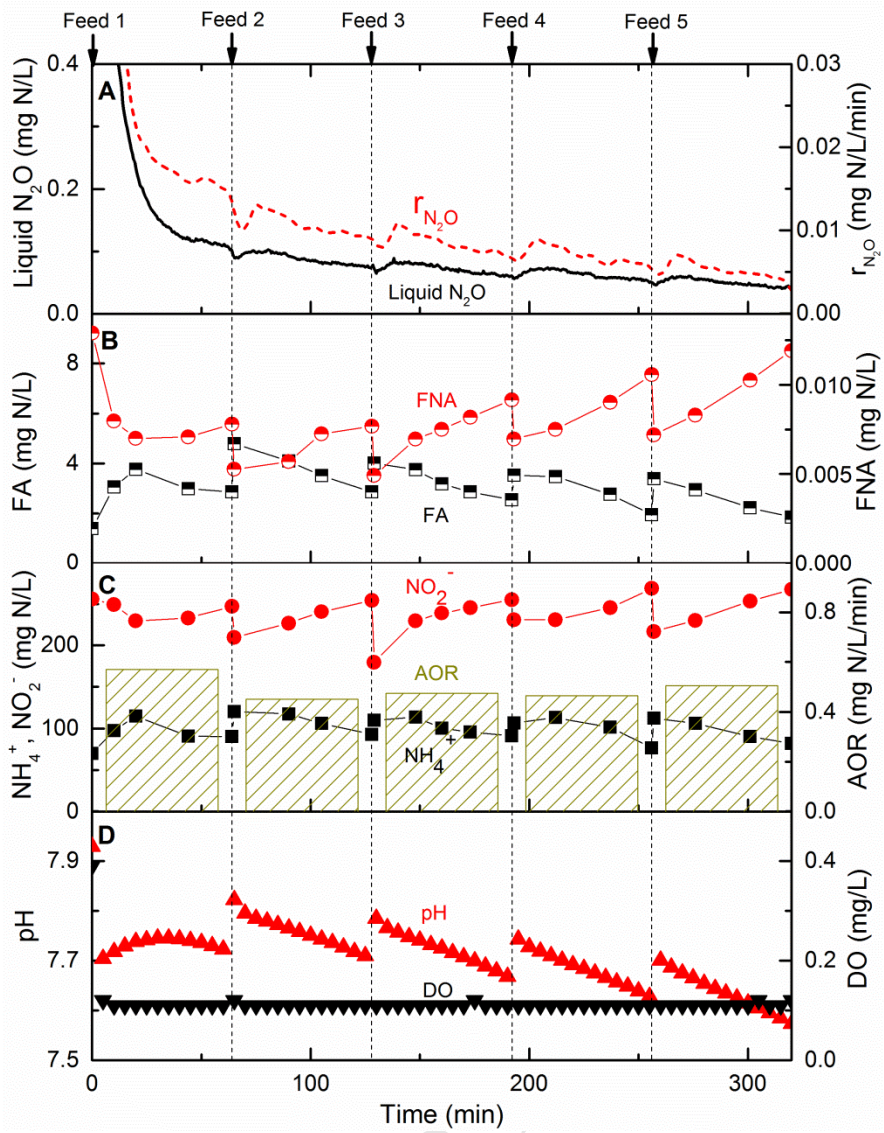

Fig. 2. In-cycle profiles of nitrogen species, pH, DO and N_2O in R1 (day 397). (A) Liquid N_2O concentrations and net N_2O production rates. (B, C) Bulk liquid nitrogen species (NO_2^- and NH_4^+), calculated free nitrous acid (FNA), free ammonia (FA) and ammonium oxidizing rates (AORs). (D) pH and DO.

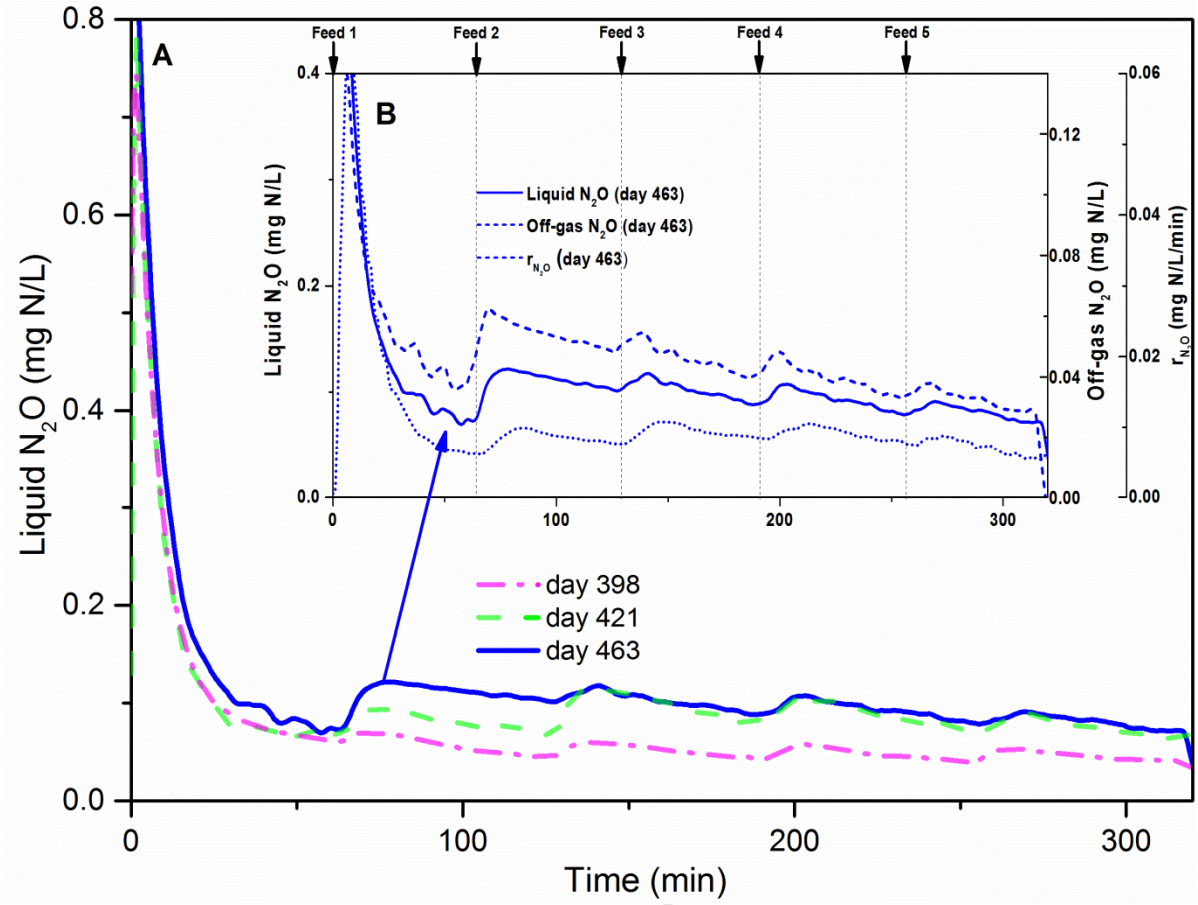

Fig. 3. (A) Profiles of liquid N_2O concentrations in one cycle in R2 on day 398, 421 and 463. (B) Profiles of liquid and off-gas N_2O concentrations and calculated net N_2O production rates in one cycle in R2 on day 463.

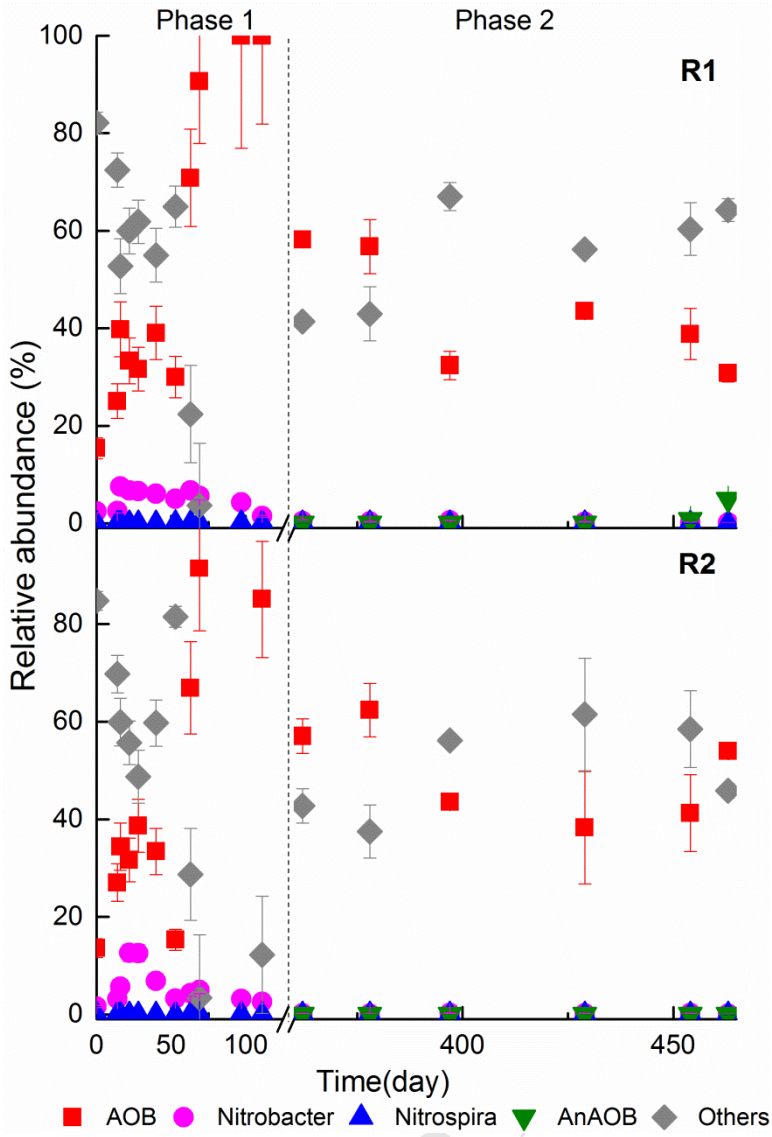

Fig. 4. Relative abundances of AOB, NOB, AnAOB and other bacteria in R1 and R2 over time based on qPCR of 16S rRNA genes. Error bars indicate standard deviations of duplicate measurements.

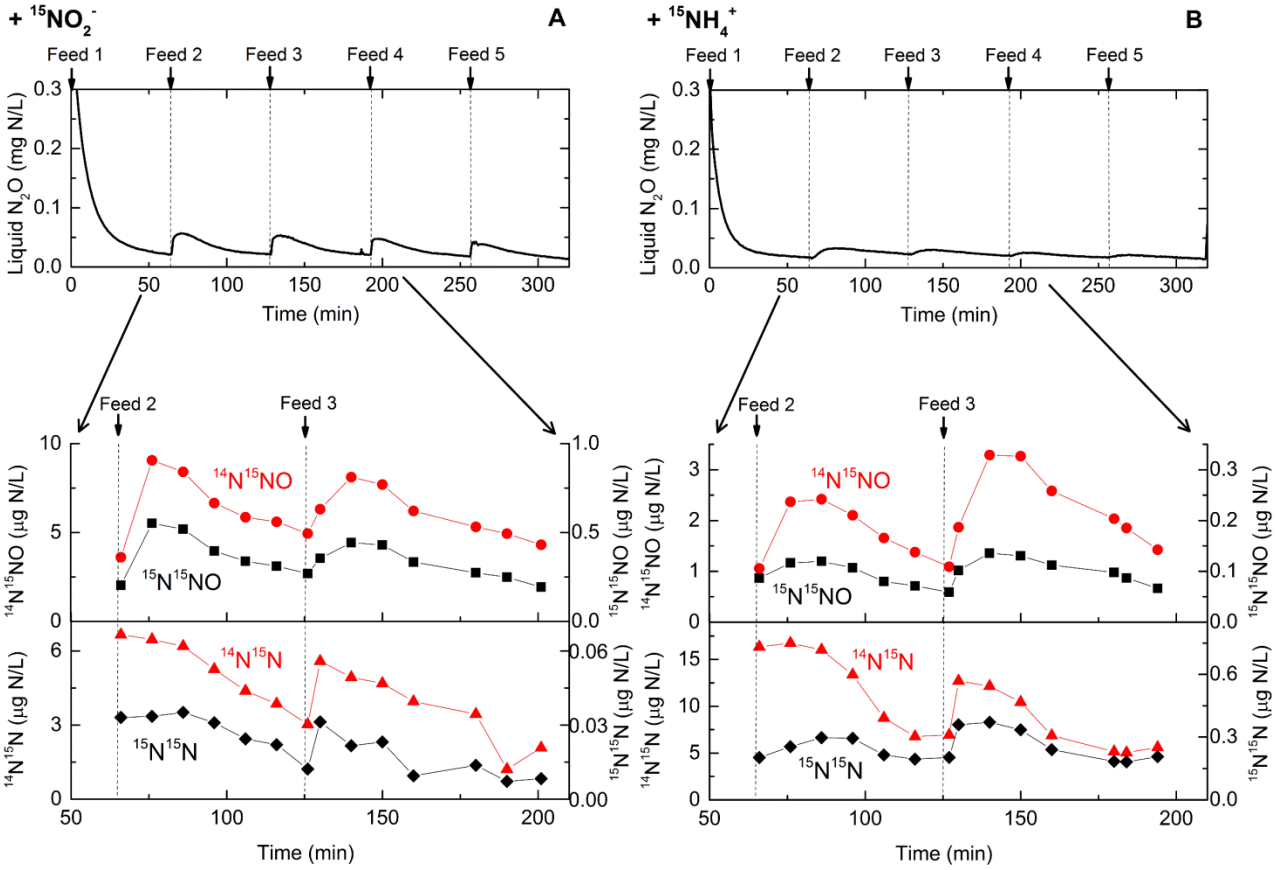

Fig. 5. Plots of bulk liquid N_2O concentrations versus time during the reaction phase of one cycle (upper panels) and isotopically labeled N_2O and N_2 concentrations versus time for feed 2 and 3 (lower panels) in Reactor 1. $^{15}NO_2^-$ spikes were performed at 111 days of operation (A) and $^{15}NH_4^+$ spikes at 107 days of operation (B).

Highlights

- Long-term high nitritation performance was achieved in intermittently-fed SBRs.
- Net N_2O production was, on average, 2.1% of the oxidized ammonium.
- Intermittent feeding appears an effective approach to mitigate N_2O emission.
- pH has a potential stimulatory effect on N_2O production.
- Nitrifier denitrification was the dominant source of N_2O production.